From Fig. 10, at a constant value of θ_m, as β increases, d_{eq} decreases. At the end of the curve, the β is denoted by β_e. When $\beta > \beta_e$, (6)–(12) have no solution. At $\beta = \beta_e$, the d_{eq} does not decrease to zero, which means that one can not find an antenna system without cross polarization by means of tilting the hyperboloid axis to the paraboloid axis. Another technique should be used. In high-power antenna systems, the transmission and the reception can use a common reflector antenna with a duplexing grid placed between the transmission horn and the subreflector, by which the cross polarization component will be filtered through, so that, it does not affect the receiver.

With the method here, it is convenient to study the changes of the antenna's electrical characteristics and geometrical dimensions with the changes of the starting parameters.

References

[1] Y. Rahmat-Smaii, D.-W. Duan, D. V. Giri, and L. F. Libelo, "Canonical examples of reflector antennas for high-power microwave applications," *IEEE Trans. Electromag. Compat.*, vol. 34, pp. 197–205, Aug. 1992.

[2] C. Dragone, "Offset multireflector antennas with perfect pattern symmetry and polarization discrimination," *Bell Syst. Tech. J.*, vol. 57, no. 7, pp. 2663–2684, Sept. 1978.

[3] Y. Rahmat-Samii and V. Galindo-Israel, "Scan performance of dual offset reflector antennas for satellite communications," *Radio Sci.*, vol. 16, no. 6, pp. 1093–1099, Nov./Dec. 1981.

[4] R. A. Shore, "A simple derivation of the basic design equation for offset dual reflector antennas with rotational symmetry and zero cross polarization," *IEEE Trans. Antennas Propagat.*, vol. AP-33, no. 1, pp. 114–116, June 1985.

[5] K. W. Brown and A. Prata, Jr., "A design procedure for classical offset dual reflector antennas with circular aperture," *IEEE Trans. Antennas Propagat.*, vol. 42, pp. 1145–1153, Aug. 1994.

[6] W. A. Imbriale, D. J. Hoppe, M. S. Esquivel, and B. L. Conroy, "A beamwaveguide design for high-power applications," *SPIE, Intense Microwave and Particle Beams*, vol. SPIE-1629, pp. 310–318, 1992.

[7] K. R. Goudey and A. F. Sciambi, "High-power X-band monopulse tracking feed for the Lincoln Laboratory long-range imaging radar," *IEEE Trans., Microwave Theory Tech.*, vol. MTT-26, pp. 326–331, May 1978.

[8] S. B. Conh, "Flare-angle changes in a horn as a means of pattern control," *Microwave J.*, pp. 41–46, Oct. 1970.

[9] D. W. Metzger, J. D. Norgard, and R. M. Sega, "Near-field patterns from pyramiclal horn antennas: Numerical calculation and experimental verification," *IEEE Trans. Electromag. Compat.*, vol. 33, pp. 188–196, Aug. 1991.

[10] Y. Rahmat-Samii, "Reflector antennas," *Antenna Handbook*, 1988, ch. 15.

[11] W. V. T. Rusch, A. Prata, Jr., Y. Rahmat-Smaii, and R. A. Shone, "Derivation and application of the equivalent paraboloid for classical offset Cassegrain and Gregorian antennas," *IEEE Trans. Antennas Propagat.*, vol. 38, pp. 1141–1149, Aug. 1990.

Shielding Effectiveness of Single and Double Plates with Slits

Jean-Fu Kiang

***Abstract*—Transverse electric (TE) wave transmission through slits on single and double metal plates of finite thickness is studied by using the Galerkin's method. It is observed that by either using a thick plate (for slit narrower than half a wavelength) or using double plates with slits laterally shifted (for slits wider than half a wavelength), the amount of power transmitted through the slits can be significantly reduced. These schemes can be applied to improve the shielding effectiveness of equipment cabinet.**

***Index Terms*—Galerkin's method, shielding, slits.**

I. Introduction

Electromagnetic wave scattering by and transmission through slots or holes on metal screens is an important subject in electromagnetic compatibility [1]. The scattering properties of certain regular holes on a plate of zero thickness can be described by using equivalent electric and magnetic dipoles [2]. To characterize large slots or slots on a thick plate, the detailed field distributions in and around the slots need to be considered. For plate of zero thickness, method of moments has been used to solve for the characteristic modes of a finite-length slot [3]. In [4], Gaussian elementary beams are used to expand the equivalent magnetic surface current across a slot, where the field distribution away from the slot can be obtained directly.

For slits on thick plates, finite difference time domain (FDTD) method has been proposed to explore the properties of lapped joints and slots at junctions of metal plates [5], and narrow apertures of finite depth [6]. Moment methods have also been used to calculate the transmission through a filled slot [7] and the characteristic modes in the slot [8]. In [9], a mode-matching technique combined with Fourier transform is proposed to study the scattering and transmission properties of a slit. In [10], a finite element and boundary integral method is used to study the scattering and transmission properties of an inhomogeneously filled slot of irregular shape. The resonance depth of slits has been discussed in [5], and it can be used to detect the presence of narrow slits [11].

In most of these studies, less attention has been paid to the shielding effectiveness of narrow slits existing in almost all equipment cabinets. In this paper, we will analyze the shielding effectiveness of single and double plates against an incident transverse electric (TE) plane wave when slits exist. A Galerkin's method will be developed to calculate the transmission cross sections of slits on thick plates.

II. Formulation

The cross section of slits on single and double thick metal plates are shown in Fig. 1. All slits are assumed to have an infinite length in the y direction. A plane wave is incident upon the plate with an angle θ_i, and an equivalent problem is formed in each region. The gap in the boundary between two contiguous regions is replaced by a perfect electric conductor and a magnetic surface current associated with the tangential electric field. The field distribution in each region can be

Manuscript received November 18, 1996; revised June 16, 1997. This work was supported in part by the National Science Council of the R.O.C. under Contract NSC-86-2221-E005-011.

The author is with the Department of Electrical Engineering, National Chung-Hsing University, Taichung, Taiwan, R.O.C.

Publisher Item Identifier S 0018-9375(97)06433-8.

expressed in terms of these equivalent magnetic surface currents. Then, impose the boundary condition that the tangential magnetic fields are continuous across the gaps. The resulting equations are then solved by using the Galerkin's method. Only the TE wave case is considered in this paper, the TM wave case is being studied, and will be published later.

A. Slit on Single Plate

A TE wave is incident upon the slit with an angle θ_i. The field components are $\overline{E}^i = \hat{y}E_o e^{ik_0(x\sin\theta_i - z_0\cos\theta_i)}$ and $\overline{H}^i = (E_o/\eta_o)(\hat{x}\cos\theta_i + \hat{z}\sin\theta_i)e^{ik_0(x\sin\theta_i - z_0\cos\theta_i)}$ where $k_0 = \omega\sqrt{\mu_o\epsilon_o}$, $\eta_o = \sqrt{\mu_o/\epsilon_o}$, and $z_0 = z + d_0$. The time convention of $e^{-i\omega t}$ is assumed. Higher order TE modes are induced inside the slit. The fields in each region can be expressed as

$$\begin{aligned}
E_{0y} &= E_o[e^{ik_0(x\sin\theta_i - z_0\cos\theta_i)} - e^{ik_0(x\sin\theta_i + z_0\cos\theta_i)}] \\
&\quad + \int_{-\infty}^{\infty} dk_x e^{ik_x x + ik_{0z}z_0} e_0(k_x) \\
H_{0x} &= \left(\frac{E_o}{\eta_o}\right)\cos\theta_i[e^{ik_0(x\sin\theta_i - z_0\cos\theta_i)} \\
&\quad + e^{ik_0(x\sin\theta_i + z_0\cos\theta_i)}] \\
&\quad - \int_{-\infty}^{\infty} dk_x e^{ik_x x + ik_{0z}z_0}\frac{k_{0z}}{\omega\mu_o} e_0(k_x) \\
E_{1y} &= \sum_{n=1}^{\infty}\sin\alpha_n x[e_n^{(1a)}\sin\gamma_{1n}z_1 \\
&\quad + e_n^{(1b)}\sin\gamma_{1n}(z_1 - h_1)] \\
H_{1x} &= -\sum_{n=1}^{\infty}\sin\alpha_n x\frac{\gamma_{1n}}{i\omega\mu_o}[e_n^{(1a)}\cos\gamma_{1n}z_1 \\
&\quad + e_n^{(1b)}\cos\gamma_{1n}(z_1 - h_1)] \\
E_{2y} &= \int_{-\infty}^{\infty} dk_x e^{ik_x x - ik_{2z}z_2} e_2(k_x) \\
H_{2x} &= \int_{-\infty}^{\infty} dk_x e^{ik_x x - ik_{2z}z_2}\frac{k_{2z}}{\omega\mu_o} e_2(k_x)
\end{aligned} \tag{1}$$

where $z_1 = z + d_1$, $z_2 = z + d_1$, $h_1 = d_1 - d_0$ is the thickness of the plate, $\alpha_n = n\pi/a$, $\alpha_n^2 + \gamma_{1n}^2 = \omega^2\mu_o\epsilon_1$, $k_{iz} = \sqrt{k_0^2 - k_x^2}$ for $i = 0, 2$. The first term in the E_{0y} and H_{0x} expressions represents the incident and the reflected TE waves, the integrals in the E_{0y} and H_{0x} expressions are the contribution by the induced magnetic surface current $\overline{M}_0$. By using the equivalence $\overline{M} = \overline{E}\times\hat{n}$ at the gaps, we obtain the following relations between the unknown coefficients and the Fourier transform of the magnetic surface current

$$\begin{aligned}
e_0(k_x) &= M_{0x}(k_x) \\
e_2(k_x) &= M_{1x}(k_x) \\
e_n^{(1a)} &= \frac{M_{0n}}{\sin\gamma_{1n}h_1} \\
e_n^{(1b)} &= -\frac{M_{1n}}{\sin\gamma_{1n}h_1}, \qquad 1 \le n < \infty
\end{aligned} \tag{2}$$

where

$$\begin{aligned}
M_{ix}(k_x) &= \frac{1}{2\pi}\int_{-\infty}^{\infty} dx e^{-ik_x x} M_{ix}(x) \\
M_{in} &= \frac{2}{a}\int_0^a dx\sin\alpha_n x M_{ix}(x) \\
&\quad i = 0, 1.
\end{aligned} \tag{3}$$

The magnetic fields can be expressed in terms of the Fourier transform of the magnetic surface currents by substituting (2) into (1).

Next, impose the boundary conditions that the tangential magnetic fields are continuous across the gaps at $z = -d_0$ and $z = -d_1$ to obtain two equations with the magnetic surface currents as unknowns. To apply the Galerkin's method, first choose a set of basis functions to represent the magnetic surface currents as

$$M_{ix}(x) = \sum_{p=1}^{N_i} u_{ip} f_{ip}(x), \qquad i = 0, 1 \tag{4}$$

where u_{ip}'s are the unknown coefficients, and $f_{ip}(x)$'s are the basis functions

$$f_{ip}(x) = x(x-a)T_p\left[\frac{\left(x - \frac{a}{2}\right)}{\left(\frac{a}{2}\right)}\right], \qquad i = 0, 1 \tag{5}$$

where $T_p(x)$ is the pth order Chebyshev polynomial. Next, take the Fourier transform of (4) according to (3), then substitute them into the two equations just obtained. Choose the same set of basis functions as the weighting functions, and take the inner product of these weighting functions with the two equations to have

$$\begin{aligned}
&\frac{2E_o}{\eta_o}\cos\theta_i\int_0^a dx e^{ik_0 x\sin\theta_i} f_{0q}(x) \\
&\quad - \sum_{p=1}^{N_0} u_{0p} 2\pi\int_{-\infty}^{\infty} dk_x f_{0q}(-k_x)\frac{k_{0z}}{\omega\mu_o} f_{0p}(k_x) \\
&= -\sum_{p=1}^{N_0} u_{0p}\sum_{n=1}^{\infty}\frac{a}{2} f_{0q,n}\frac{\gamma_{1n}}{i\omega\mu_o}\cot\gamma_{1n}h_1 f_{0p,n} \\
&\quad + \sum_{p=1}^{N_1} u_{1p}\sum_{n=1}^{\infty}\frac{a}{2} f_{0q,n}\frac{\gamma_{1n}}{i\omega\mu_o}\csc\gamma_{1n}h_1 f_{1p,n} \\
&\quad 1 \le q \le N_0
\end{aligned}$$

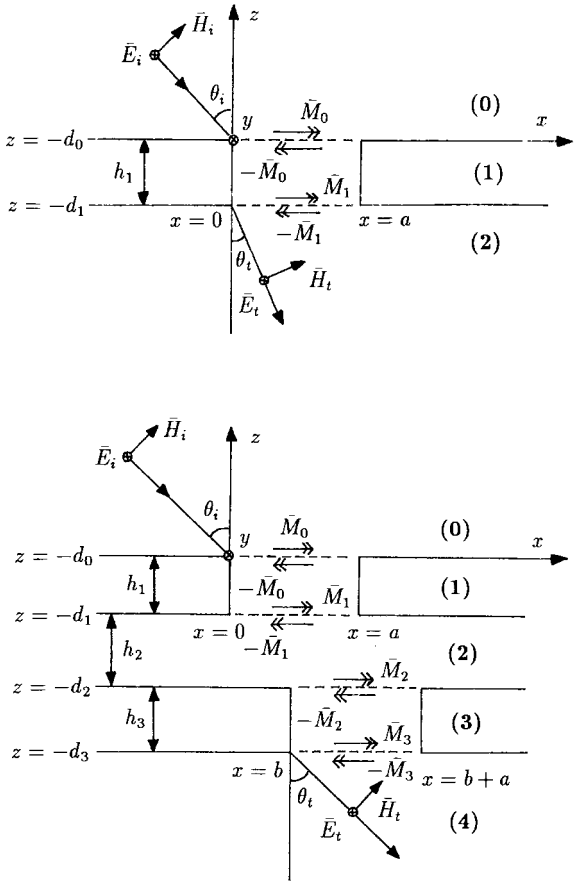

Fig. 1. Configurations of slits on single and double plates of finite thickness.

$$\sum_{p=1}^{N_1} u_{1p} 2\pi \int_{-\infty}^{\infty} dk_x f_{1q}(-k_x) \frac{k_{2z}}{\omega\mu_o} f_{1p}(k_x)$$
$$= -\sum_{p=1}^{N_0} u_{0p} \sum_{n=1}^{\infty} \frac{a}{2} f_{1q,n} \frac{\gamma_{1n}}{i\omega\mu_o} \csc\ \gamma_{1n} h_1 f_{0p,n}$$
$$+ \sum_{p=1}^{N_1} u_{1p} \sum_{n=1}^{\infty} \frac{a}{2} f_{1q,n} \frac{\gamma_{1n}}{i\omega\mu_o} \cot\ \gamma_{1n} h_1 f_{1p,n}$$
$$1 \le q \le N_1 \tag{6}$$

where

$$f_{ip}(k_x) = \frac{1}{2\pi} \int_{-\infty}^{\infty} dx e^{-ik_x x} f_{ip}(x)$$
$$f_{ip,n} = \frac{2}{a} \int_0^a dx \sin\ \alpha_n x f_{ip}(x)$$
$$i = 0, 1; 1 \le p \le N_i. \tag{7}$$

The integrals in (7) are implemented numerically. Once the unknown coefficients u_{ip}'s are solved from (6), the field in each region can be obtained from (1).

B. Slits on Double Plates

For slits on double thick plates shown in Fig. 1, the magnetic fields in each region can be expressed in terms of the Fourier transform of the equivalent magnetic surface currents as

$$H_{0x} = \left(\frac{E_o}{\eta_o}\right) \cos\ \theta_i [e^{ik_0(x \sin\ \theta_i - z_0 \cos\ \theta_i)} + e^{ik_0(x \sin\ \theta_i + z_0 \cos\ \theta_i)}] - \int_{-\infty}^{\infty} dk_x e^{ik_x x + ik_{0z} z_0} \frac{k_{0z}}{\omega\mu_o} M_{0x}(k_x)$$
$$H_{1x} = -\sum_{n=1}^{\infty} \sin\ \alpha_n x \frac{\gamma_{1n}}{i\omega\mu_o} \left[\frac{\cos\ \gamma_{1n} z_1}{\sin\ \gamma_{1n} h_1} M_{0n} - \frac{\cos\ \gamma_{1n}(z_1 - h_1)}{\sin\ \gamma_{1n} h_1} M_{1n}\right]$$
$$H_{2x} = -\int_{-\infty}^{\infty} dk_x e^{ik_x x} \frac{k_{2z}}{i\omega\mu_o} \left[\frac{\cos\ k_{2z} z_2}{\sin\ k_{2z} h_2} M_{1x}(k_x) - \frac{\cos\ k_{2z}(z_2 - h_2)}{\sin\ k_{2z} h_2} M_{2x}(k_x)\right]$$
$$H_{3x} = -\sum_{n=1}^{\infty} \sin\ \alpha_n (x - b) \frac{\gamma_{3n}}{i\omega\mu_o} \left[\frac{\cos\ \gamma_{3n} z_3}{\sin\ \gamma_{3n} h_3} M_{2n} - \frac{\cos\ \gamma_{3n}(z_3 - h_3)}{\sin\ \gamma_{3n} h_3} M_{3n}\right]$$
$$H_{4x} = \int_{-\infty}^{\infty} dk_x e^{ik_x x - ik_{4z} z_4} \frac{k_{4z}}{\omega\mu_o} M_{3x}(k_x) \tag{8}$$

where $\alpha_n = n\pi/a$, $\alpha_n^2 + \gamma_{in}^2 = \omega^2\mu_o\epsilon_i$ with $i = 1, 3$, $k_x^2 + k_{iz}^2 = \omega^2\mu_o\epsilon_i$ with $i = 0, 2, 4$. The Fourier transform of the magnetic surface currents are defined as

$$M_{ix}(k_x) = \frac{1}{2\pi} \int_{-\infty}^{\infty} dx e^{-ik_x x} M_{ix}(x)$$
$$M_{in} = \frac{2}{a} \int_0^a dx_i \sin\ \alpha_n x_i M_{ix}(x), \qquad 0 \le i \le 3 \tag{9}$$

where $x_0 = x_1 = x$ and $x_2 = x_3 = x - b$. Expand the magnetic surface currents in terms of a set of basis functions as in (4) with $i = 0, 1, 2, 3$. Substitute the magnetic surface current expansion into (8), then impose the boundary conditions that the tangential magnetic fields are continuous across the gaps. Applying the Galerkin's procedure, we obtain

$$\frac{2E_o}{\eta_o} \cos\ \theta_i \int_0^a dx e^{ik_{0x} \sin\ \theta_i} f_{0q}(x)$$
$$- \sum_{p=1}^{N_0} u_{0p} 2\pi \int_{-\infty}^{\infty} dk_x f_{0q}(-k_x) \frac{k_{0z}}{\omega\mu_o} f_{0p}(k_x)$$
$$= -\sum_{p=1}^{N_0} u_{0p} \sum_{n=1}^{\infty} \frac{a}{2} f_{0q,n} \frac{\gamma_{1n}}{i\omega\mu_o} \cot\ \gamma_{1n} h_1 f_{0p,n}$$
$$+ \sum_{p=1}^{N_1} u_{1p} \sum_{n=1}^{\infty} \frac{a}{2} f_{0q,n} \frac{\gamma_{1n}}{i\omega\mu_o} \csc\ \gamma_{1n} h_1 f_{1p,n}$$
$$1 \le q \le N_0$$
$$- \sum_{p=1}^{N_1} u_{1p} 2\pi \int_{-\infty}^{\infty} dk_x f_{1q}(-k_x) \frac{k_{2z}}{i\omega\mu_o} \cot\ k_{2z} h_2 f_{1p}(k_x)$$
$$+ \sum_{p=1}^{N_2} u_{2p} 2\pi \int_{-\infty}^{\infty} dk_x f_{1q}(-k_x) \frac{k_{2z}}{i\omega\mu_o} \csc\ k_{2z} h_2 f_{2p}(k_x)$$
$$= -\sum_{p=1}^{N_0} u_{0p} \sum_{n=1}^{\infty} \frac{a}{2} f_{1q,n} \frac{\gamma_{1n}}{i\omega\mu_o} \csc\ \gamma_{1n} h_1 f_{0p,n}$$
$$+ \sum_{p=1}^{N_1} u_{1p} \sum_{n=1}^{\infty} \frac{a}{2} f_{1q,n} \frac{\gamma_{1n}}{i\omega\mu_o} \cot\ \gamma_{1n} h_1 f_{1p,n}$$
$$1 \le q \le N_1$$
$$- \sum_{p=1}^{N_1} u_{1p} 2\pi \int_{-\infty}^{\infty} dk_x f_{2q}(-k_x) \frac{k_{2z}}{i\omega\mu_o} \csc\ k_{2z} h_2 f_{1p}(k_x)$$
$$+ \sum_{p=1}^{N_2} u_{2p} 2\pi \int_{-\infty}^{\infty} dk_x f_{2q}(-k_x) \frac{k_{2z}}{i\omega\mu_o} \cot\ k_{2z} h_2 f_{2p}(k_x)$$
$$= -\sum_{p=1}^{N_2} u_{2p} \sum_{n=1}^{\infty} \frac{a}{2} f_{2q,n} \frac{\gamma_{3n}}{i\omega\mu_o} \cot\ \gamma_{3n} h_3 f_{2p,n}$$
$$+ \sum_{p=1}^{N_3} u_{3p} \sum_{n=1}^{\infty} \frac{a}{2} f_{2q,n} \frac{\gamma_{3n}}{i\omega\mu_o} \csc\ \gamma_{3n} h_3 f_{3p,n}$$
$$1 \le q \le N_2$$
$$\sum_{p=1}^{N_3} u_{3p} 2\pi \int_{-\infty}^{\infty} dk_x f_{3q}(-k_x) \frac{k_{4z}}{\omega\mu_o} f_{3p}(k_x)$$
$$= -\sum_{p=1}^{N_2} u_{2p} \sum_{n=1}^{\infty} \frac{a}{2} f_{3q,n} \frac{\gamma_{3n}}{i\omega\mu_o} \csc\ \gamma_{3n} h_3 f_{2p,n}$$
$$+ \sum_{p=1}^{N_3} u_{3p} \sum_{n=1}^{\infty} \frac{a}{2} f_{3q,n} \frac{\gamma_{3n}}{i\omega\mu_o} \cot\ \gamma_{3n} h_3 f_{3p,n}$$
$$1 \le q \le N_3 \tag{10}$$

where

$$f_{ip}(k_x) = \frac{1}{2\pi} \int_{-\infty}^{\infty} dx e^{-ik_x x} f_{ip}(x)$$
$$f_{ip,n} = \frac{2}{a} \int_0^a dx \sin\ \alpha_n x_i f_{ip}(x)$$
$$0 \le i \le 3; 1 \le p \le N_i. \tag{11}$$

Once the unknown coefficients u_{ip}'s are solved from (10), the field in each region can be obtained from (8).

III. Numerical Results

First, consider a plane wave incident upon a thick plate with a slit. The magnitude of $M_{0x}(x)$ and $M_{1x}(x)$ are shown in Fig. 2. Our results match reasonably well with the results from [7].

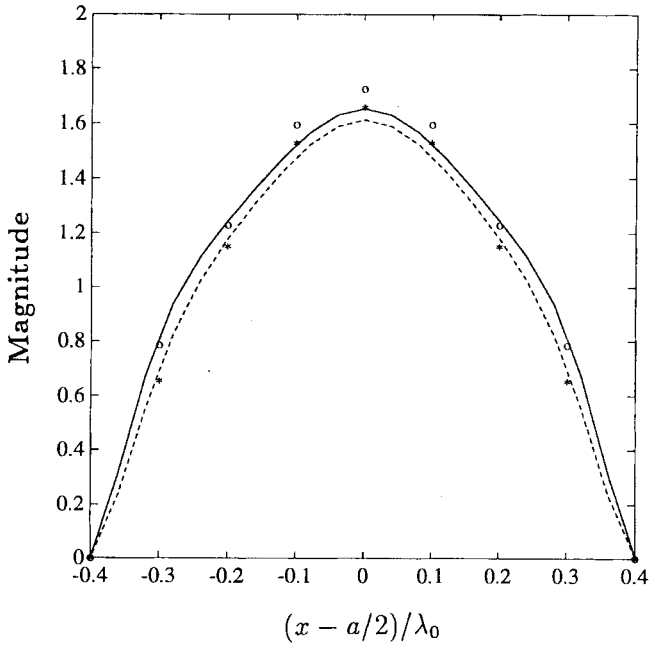

Fig. 2. Magnitude of magnetic surface currents on both sides of a slit on a thick plate, $\theta_i = 0$, $a = 0.8\ \lambda_0$, $h_1 = 0.2\ \lambda_0$, $\epsilon_1 = \epsilon_o$, ——: $M_{0x}(x)$, – – –: $M_{1x}(x)$, ∘: $M_{0x}(x)$ from [7], ∗: $M_{1x}(x)$ from [7].

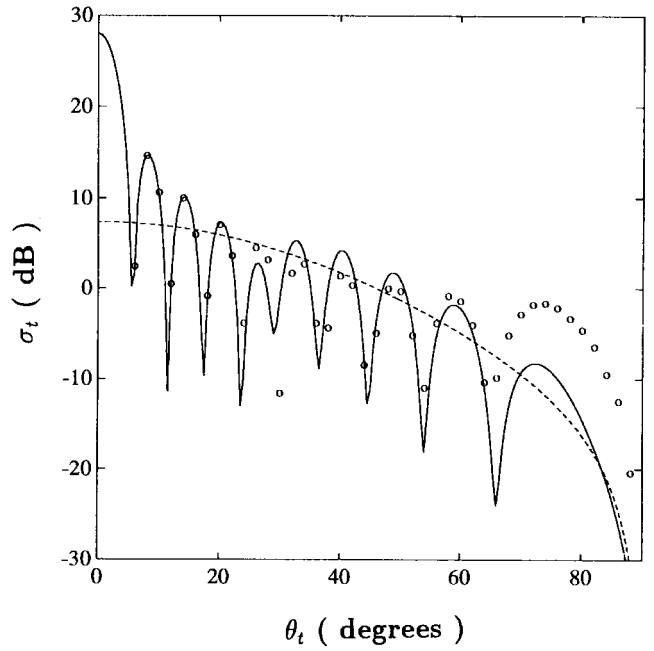

Fig. 3. Transmission cross section through a slit on a thick plate, $\theta_i = 0$, $\epsilon_1 = \epsilon_o$, ——: $a = 10\ \lambda_0$, $h_1 = 0.001\ \lambda_0$, – – –: $a = \lambda_0$, $h_1 = 0.25\ \lambda_0$, ∘: results from [9].

Fig. 3 shows the transmission cross section of a plane wave incident upon the slit, which is defined as

$$\sigma_t(\theta_t,\ \theta_i) = 10\ \log_{10}\left[2\pi\rho\frac{|E_{2y}(\overline{\rho})|^2}{|E_o|^2}\right]_{\text{dB}}. \tag{12}$$

Our results with $a = 10\lambda_0$ match well with those of [9] in $0 \le \theta_i \le 60^\circ$. The field computation near grazing angles is more dependent on the approaches used. The results by the integral equation method developed in this paper, by the mode-matching method used in [9], and by the Keller's method cited in [9] are different from one another in the region $\theta_t > 60^\circ$. As the slit width is reduced to $a = \lambda_0$, all

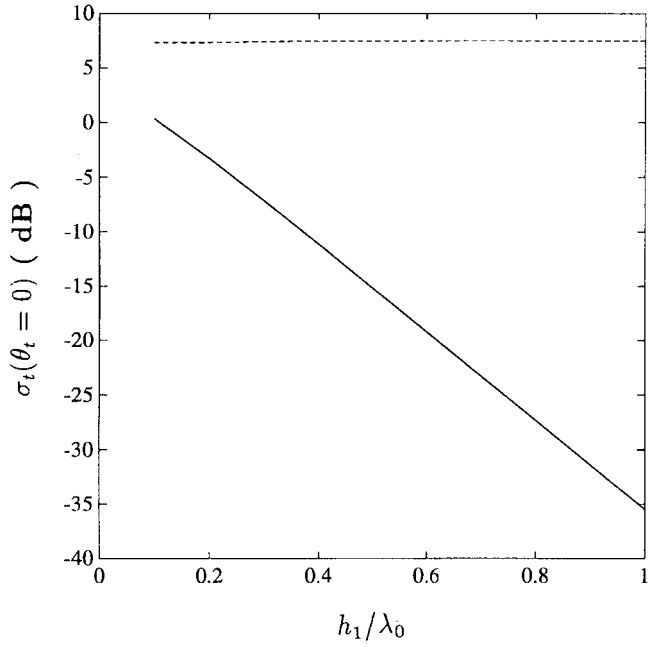

Fig. 4. Effects of slit thickness on the transmission cross section, $\theta_i = 0$, $\epsilon_1 = \epsilon_o$, – – –: $a = \lambda_0$, ——: $a = 0.4\ \lambda_0$.

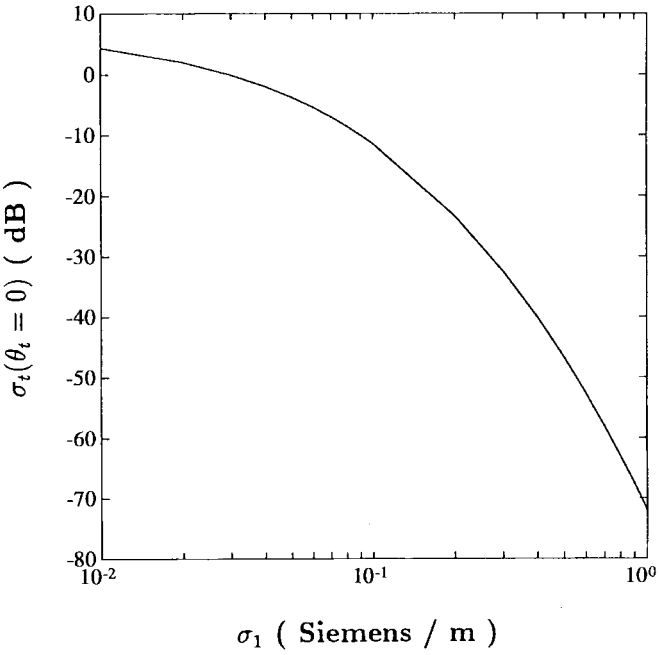

Fig. 5. Effects of slit conductivity on the transmission cross section, $\theta_i = 0$, $a = \lambda_0$, $h_1 = 0.25\lambda_0$, $\epsilon_1 = 5\epsilon_o$.

the nulls except that at $\theta_t = 90^\circ$ disappear, and the magnitude in the forward direction is reduced by about 20 dB. The transmission cross section at $\theta_t = 0$ can be used to characterize the amount of wave penetration through the slit.

Next, we show the effects of plate thickness on the transmission cross section $\sigma_t(\theta_t = 0)$ in Fig. 4. For the slit with width $a = \lambda_0$, the cross section is insensitive to the plate thickness. But for the slit with width $a = 0.4\lambda_0$, the transmission cross section is exponentially reduced by the plate thickness. For the $a = \lambda_0$ case, the TE_1 mode in the slit induced by the incident plane wave is above cutoff, and can propagate through the slit without being attenuated. However, for the $a = 0.4\ \lambda_0$ case, all the TE modes in the slit induced by the incident

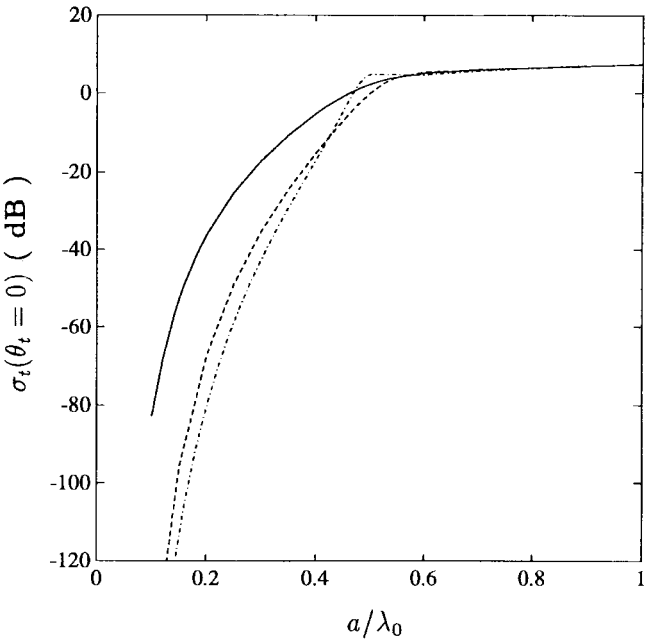

Fig. 6. Effects of slit width on the transmission cross section, $\theta_i = 0$, ——: single plate, $h_1 = 0.25\ \lambda_0, \epsilon_1 = \epsilon_o$, – – –: single plate, $h_1 = 0.5\ \lambda_0, \epsilon_1 = \epsilon_o$, –·–·–: double plates, $h_1 = h_2 = h_3 = 0.25\ \lambda_0$, $\epsilon_1 = \epsilon_2 = \epsilon_3 = \epsilon_o$.

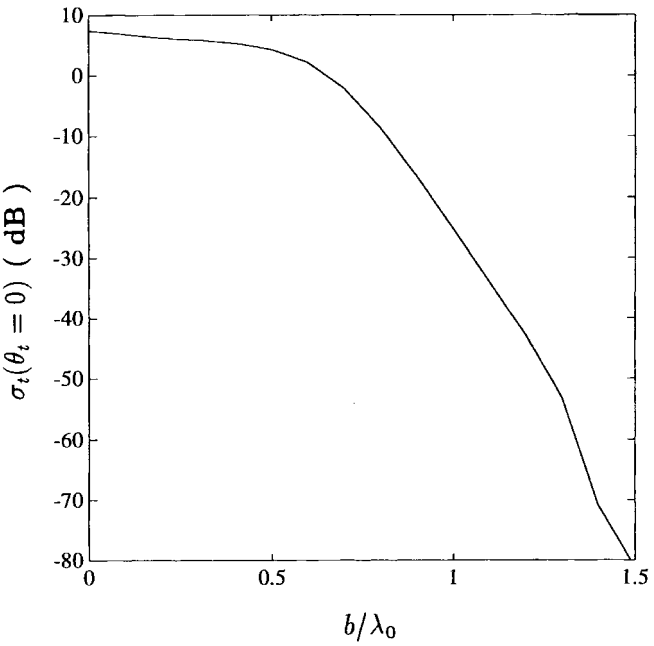

Fig. 7. Effects of lateral shift between two slits on the transmission cross section, $\theta_i = 0$, $a = \lambda_0$, $h_1 = h_2 = h_3 = 0.25\lambda_0$, $\epsilon_1 = \epsilon_2 = \epsilon_3 = \epsilon_o$.

plane wave are below cutoff, and the attenuation is exponentially related to the propagation distance which is the slit thickness. Hence, an incident TE wave can be effectively shielded by reducing the slit width to less than half a wavelength and by increasing the plate thickness.

If the slit is wider than half a wavelength, a conductive filling can be used in the slit to reduce the penetration wave. Fig. 5 shows the transmission cross section at $\theta_t = 0$ as a function of σ_1. However, for ventilation slits or slits existing in a cabinet door which need to be opened from time to time, this scheme becomes impractical or inconvenient. Hence a double plate scheme as shown in Fig. 1 is considered.

In Fig. 6, the transmission cross sections of slits on single and double plates are compared. The slits on the double plates are aligned ($b = 0$). The double plates with slits ($h_1 = h_2 = h_3 = 0.25\ \lambda_0$) have a higher shielding effectiveness than the single plate with twice the thickness ($h_1 = 0.5\lambda_0$) when the slit width is less than 0.43 wavelength. And the situation is reversed when the slit width is between 0.43 and 0.5 wavelength. For slits wider than 0.5 wavelength, none of these three schemes can shield the penetrating wave effectively.

We also study the effects of plate thickness h_1 and h_3 on the transmission cross section with the separation between plates as parameter. It is observed that increasing the plate thickness attenuates the penetrating wave exponentially, but the separation between the two plates does not have significant effect.

Finally, we show the effects of lateral shift between two slits of width λ_0 on the transmission cross section in Fig. 7. As the two slits are laterally shifted by 1.5 λ_0, the transmission cross section at $\theta_t = 0$ is reduced by more than 85 dB. This scheme does not require any conductive filling in the slits, hence can be applied to the design of cabinet ventilation to effectively shield the TE wave penetration. The results shown here represent major factors and phenomena. More results detailing other factors will be prepared in a more complete technical report later.

IV. Conclusion

A Galerkin's method has been developed to analyze the transmission properties of slits on single and double thick plates to shield an incident TE plane wave. It is observed that to effectively shield an incident TE wave, one can either increase the plate thickness (for slits narrower than half a wavelength) or use double plates with slits laterally shifted (for slits wider than half a wavelength).

Acknowledgment

The author would like to thank the reviewers for their useful comments.

References

[1] L. H. Hemming, *Architectural Electromagnetic Shielding Handbook.* New York: IEEE Press, 1992.
[2] J. Van Bladel, *Electromagnetic Fields.* New York: Hemisphere, 1985.
[3] K. Y. Kabalan, A. El-Hajj, and R. F. Harrington, "Characteristic mode analysis of a slot in a conducting plane separating different media," *IEEE Trans. Antennas Propagat.*, vol. 38, pp. 476–481, Apr. 1990.
[4] Y. Leviatan, E. Hudis, and P. D. Einziger, "A method of moments analysis of electromagnetic coupling through slots using a Gaussian beam expansion," *IEEE Trans. Antennas Propagat.*, vol. 37, pp. 1537–1544, Dec. 1989.
[5] A. Taflove, K. R. Umashankar, B. Beker, F. Harfoush, and K. S. Yee, "Detailed FD–TD analysis of electromagnetic fields penetrating narrow slots and lapped joints in thick conducting screens," *IEEE Trans. Antennas Propagat.*, vol. 36, pp. 247–257, Feb. 1988.
[6] D. J. Riley and C. D. Turner, "Hybrid thin-slot algorithm for the analysis of narrow apertures in finite-difference time-domain calculations," *IEEE Trans. Antennas Propagat.*, vol. 38, pp. 1943–1950, Dec. 1990.
[7] D. T. Auckland and R. F. Harrington, "A nonmodal formulation for electromagnetic transmission through a filled slot of arbitrary cross section in a thick conducting screen," *IEEE Trans. Microwave Theory Tech.*, vol. MTT-28, pp. 548–555, June 1980.
[8] K. Y. Kabalan, R. F. Harrington, J. R. Mautz, and H. A. Auda, "Characteristic modes for a slot in a conducting plane, TM case," *IEEE Trans. Antennas Propagat.*, vol. AP-35, pp. 331–335, Mar. 1987.
[9] S. H. Kang, H. J. Eom, and T. J. Park, "TM-scattering from a slit in a thick conducting screen: Revisited," *IEEE Trans. Microwave Theory Tech.*, vol. 41, pp. 895–899, May 1993.
[10] J.-M. Jin and J. L. Volakis, "Electromagnetic scattering by and transmission through a three-dimensional slot in a thick conducting plane," *IEEE Trans. Antennas Propagat.*, vol. 39, pp. 543–550, Apr. 1991.
[11] E. H. Newman, J. R. Birchmeier, and K. A. Shubert, "Remote detection of a thin slit in a thick ground plane," *IEEE Trans. Antennas Propagat.*, vol. AP-35, pp. 116–120, Jan. 1987.